RSC Advances

PAPER

View Article Online
View Journal | View Issue

Cite this: *RSC Adv.*, 2014, **4**, 23540

The improvement of hemostatic and wound healing property of chitosan by halloysite nanotubes

Mingxian Liu,†[a] Yan Shen,†[b] Peng Ao,[a] Libing Dai,[b] Zhihe Liu[b] and Changren Zhou*[a]

Received 13th March 2014
Accepted 29th April 2014

DOI: 10.1039/c4ra02189d

www.rsc.org/advances

As tube-like natural nanomaterials, halloysite nanotubes (HNTs) have potential applications in wound healing due to their high mechanical strength, good biocompatibility, hemostatic property, and wound healing ability. Here, we have developed flexible 3D porous chitosan composite sponges *via* the addition of HNTs. Morphological observation, mechanical property, porosity, swelling ability, and degradation behavior in phosphate buffer of the chitosan–HNTs composite sponges were investigated by various physicochemical methods. Compared to pure chitosan sponge, the composite sponges exhibit a similar porous morphology with a maximum of 8.8-fold increase in compression mechanical properties. The elastic modulus, compressive strength, and toughness of the composite sponges were simultaneously increased by HNTs. The whole-blood clotting experiment suggests that HNTs can increase the blood clotting rates of chitosan. The composite sponges with 67% HNTs shows an 89.0% increase in the clotting ability compared with pure chitosan. Cytocompatibility of the composite sponges is confirmed by cell attachment and infiltration of fibroblast and vascular endothelial cells. *In vivo* evaluation on full-thickness excision wounds in experimental Sprague-Dawley rats reveal that these composite sponges enhance the wound healing property especially at the early stage. The composite sponges show a 3.4–21-fold increase in wound closure ratio compared to that of pure chitosan after one week. The addition of HNTs helps in faster re-epithelialization and collagen deposition. All these data demonstrate the potential applications of the chitosan–HNTs composite sponges for burn wounds, chronic wounds, and diabetic foot ulcers.

1. Introduction

As the largest organ of the human body, the human skin is the first outside barrier between the body and the environment. Human skin performs many functions such as protection, sensation, control of evaporation, storage and synthesis, absorption, and water resistance. However, trauma or other injuries always lead to varying degrees of damage and skin defects. Human skin generally needs to be covered with dressings immediately after it is damaged. The wound healing can proceed through regeneration and reconstruction by a series of pathophysiological processes, which involve the complex interactions among different types of skin cells, cytokines and extracellular matrices. For the goal of wound healing, many types of dressing materials such as hydrogel,[1,2] membrane,[3,4] sponge,[5] non-woven fabrics and nanofibers[6,7] have been explored. Sponges are soft and flexible materials with interconnected microporous structure that show many unique characteristics such as good fluid absorption capability, cell interaction and hydrophilicity. However, they have some serious flaws such as low hemostasis ability, poor mechanical property, limited healing ability, and high fabrication cost, which restrict their practical applications. Many synthetic or natural macromolecules have been selected as matrices for wound dressing to improve the healing process.[8] Among these, the macromolecule, chitosan, derived from natural resources and available abundantly, is considered a promising material for tissue regeneration.[9] The desirable features of chitosan for use in wound healing include its biocompatibility, biodegradability, hemostatic activity, anti-inflectional activity and property to accelerate wound healing.[4,10] Furthermore, chitosan can easily be processed into membranes, gels, nanofibers, beads, nanoparticles, scaffolds, and sponges for wound dressing applications. Chitosan has the functions for the acceleration of infiltration of polymorphonuclear cells at the early stage of wound healing, followed by the production of collagen by fibroblasts.[11] However, the hemostatic performance, healing ability, and flexibility of chitosan should be further improved in order to expand its applications as wound dressing materials.

Clays are important adjutants and supports for medical products, since they have many physicochemical, mechanical,

[a]*Department of Materials Science and Engineering, Jinan University, Guangzhou 510632, China. E-mail: tcrz9@jnu.edu.cn*

[b]*Guangzhou Institute of Traumatic Surgery, Guangzhou Red Cross Hospital Medical College, Jinan University, Guangzhou 510220, China*

† The authors contributed equally to this work.

and biological properties such as high absorption ability, drug-loading ability, absence of toxicity, insensitive to other raw materials, and complex formation properties.[12,13] Among various types of clays, one-dimensional halloysite nanotubes (HNTs) have been used to improve the mechanical properties, drug-loading properties, cell attachment and hemostatic performance of polymers in recent years.[14] HNTs are natural inorganic nanomaterials with a chemical formula of $Al_2Si_2O_5(OH)_4 \cdot nH_2O$. The length of HNTs is in the range of 0.2–1.5 μm, while the inner diameter and the outer diameter of tubes are in the ranges of 10–40 nm and 40–70 nm, respectively. The aspect ratio (L/D) of HNTs is in the range of 10–50. The hollow lumen microstructures and porosity of HNTs afford them to have a high loading and absorption ability for active compounds;[14] therefore, HNTs are usually used in drug delivery systems and waste water treatment.[15,16] Recent research has suggested that HNTs are cytocompatible and can potentially be used as scaffold materials in tissue engineering.[17,18] These unique properties of HNTs inspire us to explore their applications in wound healing. Interestingly, in traditional Chinese medicine, halloysite (with a Chinese traditional medicine name "Chishizhi") was commonly used as wound dressing materials in the form of powder, which has been confirmed by the efficacy of hemostasis and wound healing. However, to date, there is no scientific report on the wound healing applications of HNTs. In contrast, there are numerous papers and patents on other clay minerals for use as wound dressing materials.[19–21]

Chitosan porous scaffolds prepared by lyophilization or electrospinning serve as good candidates for wound treatment with the benefit of drug/growth factors delivery.[22–25] These active compounds can significantly accelerate the wound healing process; however, the preparation process of drug-loaded chitosan scaffolds is complicated. Moreover, the loaded growth factors are easily degraded by proteinases or removed by exudate before reaching the wound bed.[22] Therefore, preparing high healing performance chitosan dressing materials loaded with drugs is still a challenge.

In the present work, the chitosan–HNTs composite sponges with different HNTs loadings were prepared by lyophilization method. The influences of HNTs on the physicochemical, microstructure, cytocompatibility, and *in vivo* wound healing ability of chitosan sponge were investigated. HNTs simultaneously improve the mechanical properties, cell attachment, hemostatic performance, and wound healing rate of chitosan. The composites sponges have a maximum of 8.8-fold increase in compression strength, an 89.0% increase in clotting ability, and a 21-fold increase in wound closure ratio compared with pure chitosan sponges. Moreover, the composite sponges have controllable porosity, swelling ratio, and degradation properties by changing the HNTs contents. In addition, the cost of the composite sponges is much lower than that of the pure chitosan sponges, which facilitates their commercialization. This work opens a new area of biomedical applications of HNTs and provides a novel routine for high performance wound dressing materials by a simple fabrication method with a low cost.

2. Experimental

2.1 Raw materials

Chitosan was purchased from Jinan Haidebei Marine Bioengineering Co. Ltd (China). Its deacetylation and viscosity-average molecular weight was 95% and 600 000 g mol^{-1}, respectively. Raw halloysite was mined from Hunan province (China) and purified before use. The elemental composition of purified HNTs by X-ray fluorescence (XRF) was as follows (wt%): SiO_2, 54.29; Al_2O_3, 44.51; Fe_2O_3, 0.63; TiO_2, 0.006. The Brunauer–Emmett–Teller (BET) surface area of the used HNTs was 50.4 m^2 g^{-1}. All other chemicals used in this work were of analytical grade. Ultrapure water from Milli-Q water system was used to prepare the aqueous solutions.

2.2 Preparation of the chitosan–HNTs composite sponge

The chitosan–HNTs composite sponges were prepared by solution mixing and subsequently by the freeze-drying method. The raw chitosan was first treated with acetic acid (2% concentration) with stirring for 10 hours. The insoluble fraction was separated by centrifugation at 8000 rpm for 15 min, and then the supernatant containing the chitosan was isolated. The purified chitosan was obtained by freeze-drying. The typical procedure to prepare the composite sponges was described below and depicted in Fig. 1. Chitosan (2 g) was dissolved in 100 mL of 2 wt% acetic acid solution under mechanical stirring. Then, the calculated amount of HNTs powder was added into the chitosan solution. The mixture was continuously stirred overnight under ambient temperature, and then treated by ultrasonic for 30 min to obtain a good dispersion of HNTs and interfacial adsorptions. Then, the solutions were poured into a cylinder plastic mold. Subsequently, they were frozen into ice at −20 °C overnight in a refrigerator, and then lyophilized at −80 °C using Christ freeze dryer ALPHA 1-2/LD plus. Then, the scaffolds were immersed for 2 h in 2% NaOH to neutralize the residual acetic acid and rinsed extensively in sterile distilled water. Finally, the scaffolds were freeze-dried and stored for further use. For comparison, pure chitosan sponge was also prepared in the same way but without the addition of HNTs. The sample codes of the composite sponge (CS2N1, CS1N1, CS1N2, CS1N4) represented the weight ratio of chitosan (CS) and HNTs (N). For example, in the CS1N2 sample the weight ratio of chitosan and HNTs was 1 : 2.

2.3 Physicochemical characterization of the chitosan–HNTs composite sponge

Scanning electron microscopy (SEM). Before SEM observation, the sponges were sectioned and sputter-coated with 10 nm thick gold–palladium layer using a sputter coater (BALTEC SCD 005). The morphology of the sponges was observed with a Philips XL30 ESEM and Hitachi S-4800 FE-SEM (for high magnification images).

Porosity. The porosity of the sponges was determined using the reported method.[26] First, the sponges were immersed in absolute ethanol until they were saturated. Afterwards, the

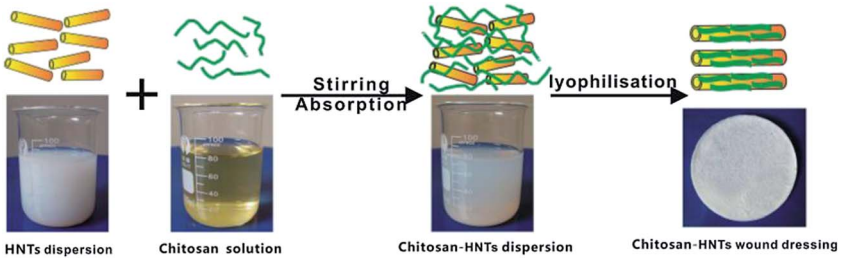

Fig. 1 Schematic representation of the preparation of chitosan–HNTs composite sponges.

sponges were weighed before and after immersion in alcohol. The porosity was calculated using the formula,

$$\text{porosity}\,(\%) = \frac{W_2 - W_1}{\rho V_1} \times \%$$

here, W_1 and W_2 are the weight of sponges before and after immersion in alcohol, respectively, V_1 is the volume before immersion in alcohol and ρ is a constant (the density of alcohol). All samples were triplicated in the experiment.

Swelling ratio. The equal volume sponges were immersed in phosphate buffered saline (PBS) (pH 7.4, 37 °C). The sponges were taken out at predetermined time intervals and the water that adhered on the surface was removed by gently blotting the sponges with filter paper. These sponges were then immediately weighed (W_d), and the swelling ratio was calculated by the following formula,

$$\text{DS}(\%) = \frac{W_w - W_d}{W_w} \times 100\%$$

here, DS is the degree of swelling, and W_w and W_d represent the wet and dry weight of the sponges, respectively.

***In vitro* biodegradation behavior.** The sponge samples were equally weighed and immersed in lysozyme (10 000 U mL^{-1}) containing the medium and incubated at 37 °C for 28 days. The samples were removed after 7, 14, 21 and 28 days from the medium containing lysozyme and washed with deionized water to remove ions adsorbed on surface and then freeze-dried. The dry weight was noted as W_t and initial weight as W_i. The degradation of the sponges was calculated using the formula,

$$\text{degradation}\,(\%) = \frac{W_i - W_t}{W_i} \times \%$$

Compression property. The compression property of pure chitosan and the chitosan–HNTs composite sponges was determined using Universal Testing Machine (Zwick/Roell Z005, Germany) at 25 °C according to ASTM D5024-95a. The samples for the test were cylinder samples with a diameter of ~16 mm and thickness of ~14 mm. The crosshead speed was 2 mm min^{-1}, and up to 85% reduction in specimen height was obtained. The stress–strain curves for every sample were recorded automatically by the testXpert® II V2.0 software. Compressive modulus was calculated as the slope of the initial linear portion of the stress–strain curves. The deformation recovery ratio (R) was calculated by the following equation,

$$R(\%) = \frac{h_f - (1-\varepsilon)h_0}{\varepsilon h_0} \times \%$$

here, h_f is the final height of sample after 30 min of the compressive testing; h_0 is the initial height of the samples before compressive testing; and ε is the deformation ratio when the compression test stops ($\varepsilon = 85\%$ for the present work). Five samples were used to obtain reliable data.

2.4 Cell cultures on the chitosan–HNTs composite sponges

Fibroblasts were isolated from a human skin biopsy and used at passages of 3–4. Endothelial cells were from a dermal microvascular origin, and keratinocyte cultures were established from human skin biopsies.

The sterile pure chitosan and chitosan–HNTs sponges were seeded with NIH 3T3 and vascular endothelial cells in a 24-well plate at a concentration of 1×10^5 cells per well. After 3 days of incubation, the sponges were washed with PBS and fixed with 2.5% glutaraldehyde for 1 h. The samples were thoroughly washed with PBS, and then sequentially dehydrated by a series of graded-ethanol solutions, freeze-dried, gold sputtered in vacuum and observed by SEM.

2.5 Whole-blood clotting and platelet activation evaluation of chitosan–HNTs composite sponges

The blood clotting study of the materials was performed according to the literature.[24,26] Blood was drawn from human ulnar vein using BD Discardit II sterile syringe and mixed with anticoagulant agent acid citrate dextrose at the ratio of 85% : 15%. Triplicate samples were determined for every sample and blood without adding materials was used as a negative control. Blood was added to 10 mg sponges and freeze-dried HNTs powder (from 5 wt% HNTs aqueous dispersion) that were placed in a 6-well plate, which was followed by the addition of 10 μL of 0.2 M $CaCl_2$ solutions to initiate blood clotting. These sponges were then incubated at 37 °C for 10 min. Fifteen milliliters (15 mL) of distilled water was then added dropwise without disturbing the clot. Subsequently, 10 mL of solution was taken from the dishes and was centrifuged at 1000 rpm for 1 min. The supernatant was collected for each sample and maintained at 37 °C for 1 hour. Two hundred microliters (200 μL) of this solution was transferred to a 96-well plate, and the optical density was measured at 540 nm using a plate reader (Multiskan MK3, Thermo Electron Corporation).

Platelet activation study was conducted as follows. Platelet-rich plasma (PRP) was isolated from the blood by centrifugation of blood at 2500 rpm for 5 min. One hundred microliters (100 μL) of PRP was poured onto the sponge piece (10 mg) and incubated at 37 °C for 20 min. The sponges were then washed three times with PBS solution and fixed using 0.1% glutaraldehyde solution. The sponges were dried and then SEM images were obtained.

2.6 *In vivo* evaluation of wound healing properties of chitosan–HNTs composite sponges

All experimental procedures were performed according to the Guide for the Care and Use of Laboratory Animals and were in compliance with the guidelines specified by the Chinese Heart Association policy on research animal use and the Public Health Service policy on the use of laboratory animals. Sprague-Dawley (SD) rats, weighing 200–250 g and 4–6 weeks of age, were used in this study. The rats were divided into seven groups and each group contains three rats ($n = 3$), and they were allowed to eat normal rat food and water without restriction. On the day of wounding, the rats were anaesthetized by intramuscular injection of 35.0 mg kg^{-1} ketamine and 5.0 mg kg^{-1} xylazine. The dorsal area of the rats was depilated and the operative area of skin cleaned with alcohol. Full thickness wounds (1.5 cm × 1.5 cm) were prepared by excising the dorsum of the rat using surgical scissors and forceps. The prepared wounds were then covered with the pure chitosan sponge, chitosan–HNTs composite sponges, commercially available adhesive wound dressing (AWD), and oily cotton gauze (OY). After applying the dressing materials, the rats were housed individually in cages at room temperature.

The dressing materials were changed at week 1, 2, and 3. During the changing of dressings, photographs were taken and the wound area was measured using a soft plastic sheet. The sheet was kept on top of the wound and the area was marked

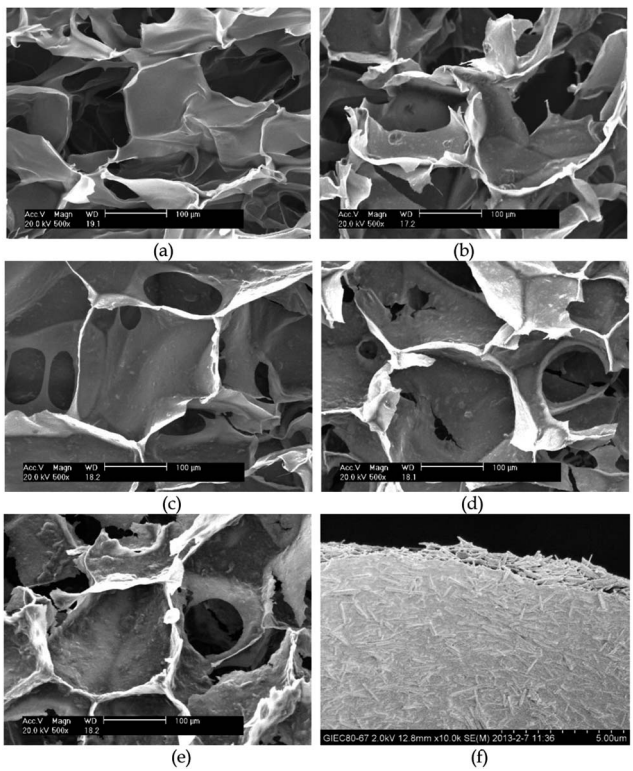

Fig. 2 SEM images of pure chitosan (a), CS2N1 (b), CS1N1 (c), CS1N2 (d), CS1N4 (e) magnified region of (c) that shows the presence of HNTs (f).

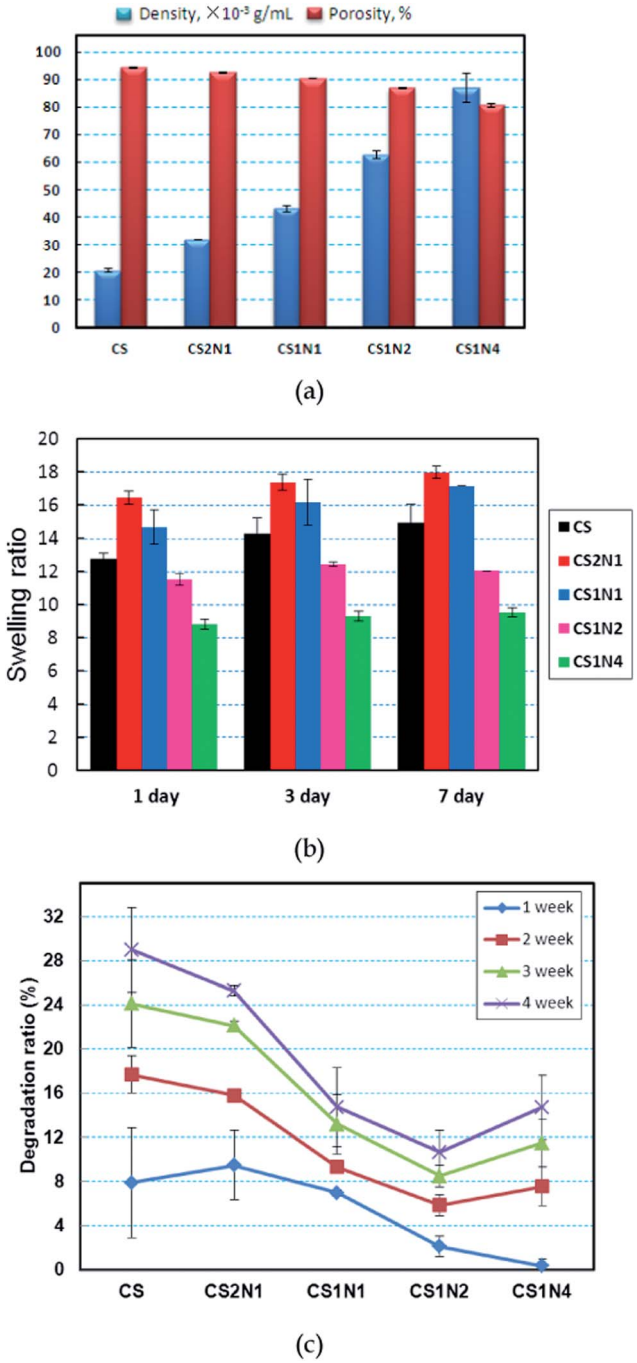

Fig. 3 Density/porosity (a), swelling ratios in PBS at 37 °C (b) and degradation ratio (c) of pure chitosan and chitosan–HNTs composite sponge.

using a marker pen. The marked area was then transferred to graph sheet to obtain the exact value. After Week 4, the wound tissue of the rat was excised, fixed with 10% formalin, and stained with a hematoxylin–eosin (H&E) reagent for histological observations. The amount and the type of collagen deposition were determined by Masson and Sirius Red (SR) staining, respectively.

3. Results and discussion

3.1 SEM observation of construction of the chitosan–HNTs composite sponges

The morphology of the lyophilized chitosan and chitosan–HNTs sponges was investigated by SEM (Fig. 2). All of the sponges show honeycomb-like porous microstructures with a pore diameter of about 200 μm and pore-wall thickness in nanometers. The addition of HNTs has a slight effect on the pore structure of the chitosan sponge even with 80 wt% HNTs loading. Such interconnected micro-pore structures of the sponges provide efficient channels for rapid liquid gas transport, benefiting their wound healing applications. In the enlarged images of the composite sponges (Fig. 2f), it is clear that HNTs are embedded in the chitosan matrix with indistinct interfaces, suggesting their strong interfacial interactions between HNTs and chitosan due to their hydrogen bonding and electrostatic attraction.[27] It should be noted that the roughness of the pore-wall for the sponges may be increased by the presence of the nanoparticles.[27–29] Moreover, the rough surface benefits the adhesion and growth of cells compared to smooth surface.[29,30] This is also confirmed in this work and will be shown in the cell experiment result below.

3.2 Physicochemical characterization of chitosan–HNTs composite sponges

The density and porosity of the prepared sponges were determined and the results are shown in Fig. 3a. As expected, the density of the chitosan–HNTs sponges increased linearly with the loading of HNTs. This is attributed to the fact that the concentration of chitosan solutions is fixed with the gradual addition of HNTs into the aqueous solution when preparing the sponges. Therefore, in the same volume of the sponges, the amount of materials in the composite sponges increases with the loading of HNTs. As a result, the density of the composite sponges increases by the addition of HNTs. The increased density of the sponges is beneficial to the improvement of mechanical properties such as dimensional stability. A slight decrease in porosity of the sponges is obtained with an increase in HNTs loadings. The pure chitosan sponges have a maximum porosity of 94.3%, while the porosity is decreased to 80.7% for the CS1N4 sponge. The porosity of the sponges is a critical factor in determining the gas permeability, fluid absorption capability, cell migration behavior, and mechanical performance. The high porosity of pure chitosan sponges is helpful in

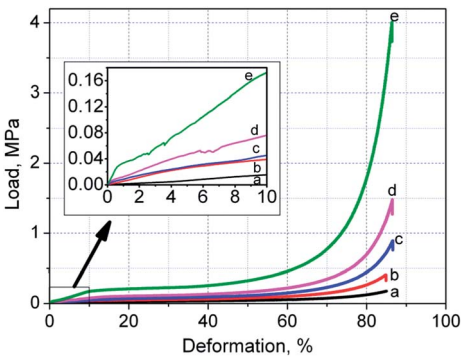

Fig. 4 Compressive stress–strain curves for chitosan–HNTs composite sponges: (a) CS; (b) CS2N1; (c) CS1N1; (d) CS1N2; (e) CS1N4. The inset shows the region for determining the compressive modulus of the samples.

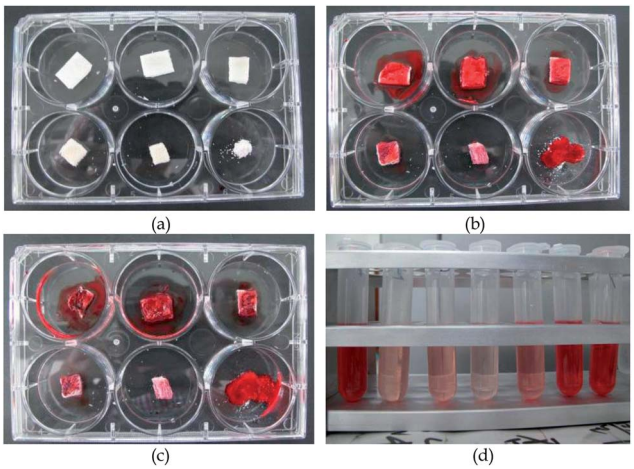

Fig. 5 Images of the sponges and freeze-dried HNTs powder (a), blood on the materials with $CaCl_2$ solution (b), clotted blood on the materials after culture at 37 °C for 30 min (c), and the corresponding aqueous solution (d). From left to right and from top to bottom: CS; CS2N1; CS1N1; CS1N2; CS1N4, HNTs powders, and blood.

Table 1 Summary of the mechanical properties data (data in the parentheses indicates the standard deviations)

Sample	Elastic modulus (kPa)	Stress at 60% strain (kPa)	Maximum load (N)	Deformation recovery ratio (%)
CS	311.7 (259.0)	55.1 (5.7)	59.9 (20.9)	9.36 (6.98)
CS2N1	408.7 (239.2)	101.0 (3.1)	75.2 (9.9)	23.11 (3.72)
CS1N1	578.3 (456.1)	151.0 (15.6)	122.0 (47.5)	30.91 (4.14)
CS1N2	1428.8 (860.2)	220.0 (10.8)	260.8 (76.2)	19.33 (4.89)
CS1N4	3054.0 (1115.5)	458.0 (24.8)	870.4 (523.6)	9.85 (5.39)

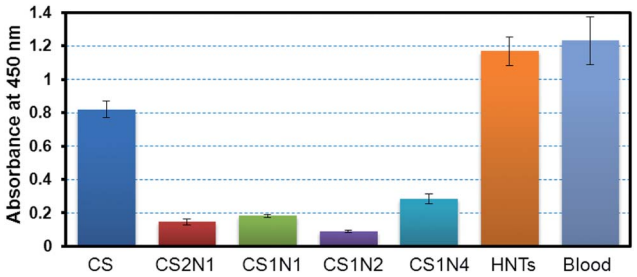

Fig. 6 Whole-blood clotting evaluation of the pure chitosan, HNTs and the chitosan–HNTs composite sponges.

absorbing exudate from the wound surface and facilitating the transfer of nutrients and medium for the cells. However, the sponges with high porosity suffer from weak stress resistance especially during compression. The influence of porosity on the mechanical performance of the sponges will be discussed in the following section.

The comparison of the swelling ratio of pure chitosan and chitosan–HNTs sponges in PBS solutions is given in Fig. 3b. On day 1, the sponges have the swelling ratios in the range of 8.8–16.4. With the extension of immersing time, all of the samples exhibit an increasing trend in the swelling ratio. For example, the swelling ratio of CS1N1 sponges increases from 14.7 on day 1 to 17.2 on day 7. With respect to the differences in swelling ratios among the samples, apart from those of pure chitosan, the swelling ratios of the composite sponges decrease with the loading of HNTs. The hydrophilicity of the materials and the pore structure of the sponges affect their swelling ratios. The decreasing degree of swelling is attributed to the low porosity, as shown in Fig. 3a, and the relatively low water absorption ability of HNTs (3–5.3%)[31] compared with the same quality of chitosan (~48%)[32] in the composite sponges. The pure chitosan sponge has a moderate swelling ratio among the samples, indicating that the water retention of the sponges can be adjusted by the addition of HNTs. The hydrophilicity of the prepared sponges is expected to accelerate the blood coagulation process and enhance cell attachment and proliferation during the tissue regeneration process.

The structural integrity of the sponges under biologically relevant pH and ion concentrations is vital to ensure sufficient maintenance of mechanical strength and porosity for cell interactions. The weight losses of the pure chitosan and chitosan–HNTs composite sponges were monitored as a measure of degradation in biological buffer (PBS) over 28 days (Fig. 3c). It can be seen that with the increase in the contact time, all of the samples decrease in weight in PBS. With incorporation of the HNTs, chitosan sponges show a decreased weight loss ratio. This is attributed to the primary degradation of the sample related to the chitosan chain breakage while HNTs almost do not degrade in PBS solutions. With the increase in the loading of HNTs, the relative contents of the chitosan in the samples decrease. As a result, the weight loss ratio of the composites is lower than that of pure chitosan. Furthermore, the interfacial interactions between HNTs and chitosan can constrain the molecular mobility of chitosan. Note that HNTs play the role of protecting chitosan against the attack by the medium. However, when the loading of HNTs is increased to 80 wt% (CS1N4), the weakened interfacial interactions may increase the chance of exposure of the chitosan chain in the medium. As a result, the CS1N4 shows a slight increase in the weight loss ratio compared with that of CS1N2. The decreased degradation rate of chitosan by the nanofillers has also been reported.[26,33,34]

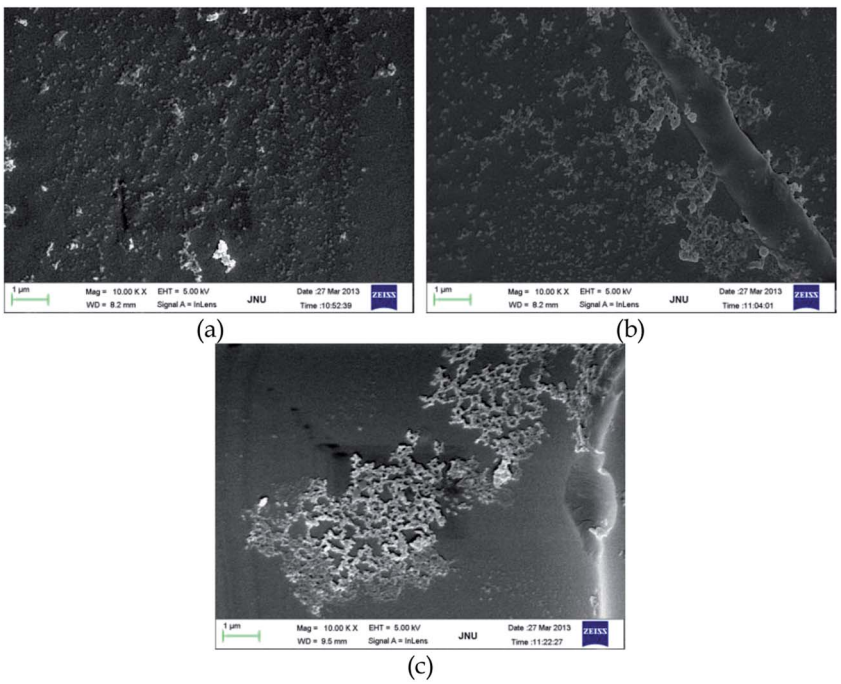

Fig. 7 SEM images of platelet activation on pure chitosan (a), CS1N1 (b), and CS1N4 (c) sponges.

3.3 Mechanical property of chitosan–HNTs composite sponges

The influences of HNTs on the mechanical properties of chitosan sponges were investigated *via* the compression test. Fig. 4 shows typical compressive stress–strain curves for pure chitosan and chitosan–HNTs composite sponges. Table 1 summarizes the data on the mechanical properties of the samples. HNTs can effectively increase the compressive modulus and strength of chitosan, and the increasing trend is proportional to the HNTs loadings. For example, the elastic modulus of CS1N4 is 3054 kPa, which is an 8.8-fold increase relative to that of pure chitosan. The reinforcing ability of HNTs for chitosan is attributed to both the high strength of the tubes and the good interfacial interactions in the composite systems as illustrated before.[17,27] Moreover, the decrease in porosity by the incorporation of HNTs also helps in improving the compression properties. On the other hand, flexibleness is critical for the practical application of wound dressing materials as well as their compression strength.[35] A material with proper flexibleness is beneficial for close contact with the wounded surface. Due to the difficulty in direct determination of impact toughness of the sponges, we employed the deformation recovery ratio to compare their flexibleness. In Table 1, all the composite sponges exhibit higher deformation recovery ratio compared with pure chitosan. The maximum deformation recovery ratio of the composite sponges (CS1N1) is three-fold compared to pure chitosan, suggesting the good elasticity of the samples. The lowered deformation recovery ratio of the composite sponges at relatively high HNTs loading (CS1N2 and CS1N4) is attributed to both the decrease of the chitosan content and the weakened interfacial interactions. All these results demonstrate that the chitosan–HNTs composite sponges can fulfill the essential requirements for dressing materials to be used on wound healing under high stresses and can provide mechanical support for the protection of wound surfaces and facilitation of cells attachment.

3.4 Evaluation of whole-blood clotting and platelet activation

In order to evaluate the influence of HNTs on the blood clotting behavior of chitosan sponges, whole blood was kept in contact

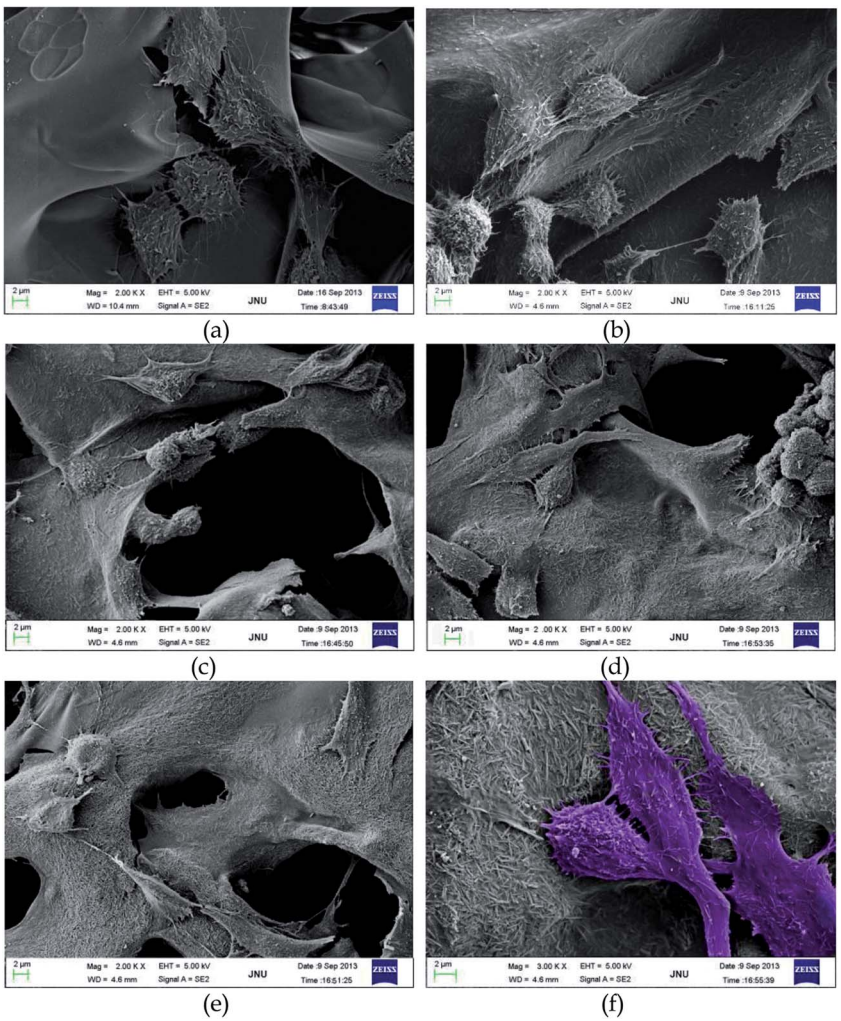

Fig. 8 SEM images of fibroblast (NIH3T3) cultured on CS–HNTs nanocomposite scaffolds after 3 days: (a) CS; (b) CS2N1; (c) CS1N1; (d) CS1N2; (e) CS1N4; (f) enlarged image of CS1N2 sample with artificial staining showing the cells.

with the prepared sponges. For comparison, the freeze-dried HNTs powder was selected as control. The appearance of the blood clot caused by the sponges and HNTs powder is shown in Fig. 5. It can be seen that the chitosan–HNTs composite sponges have much higher blood clotting ability compared with pure chitosan or neat HNTs. When the blood is dripped onto the composite sponges, the blood can be rapidly absorbed in the porous composite sponges. However, for the pure chitosan sponges and HNTs powder, the blood seems to have hardly infiltrated the material. To quantify the clotting ability of the samples, red blood cells (RBCs) that were not trapped in the sponges and the HNTs were hemolyzed with water, and the absorbance of the resulting hemoglobin solution was measured (Fig. 6). A higher absorbance value of the hemoglobin solution thus indicates a slower clotting performance. All of the composite sponges exhibit lowered absorbance than that of the pure chitosan sponge. For example, the CS2N1 and CS1N2 sponges show an 82.2% and 89.0% decrease in the absorbance value, respectively, compared with pure chitosan, suggesting their high clotting ability. However, in a similar research, adding nano-sized ZnO has nearly no effect on the clotting properties of chitosan and β-chitin.[26,36] Incorporation of nano chondroitin sulfate into chitosan–hyaluronan blend can lead to ~50% decrease in the absorbance value of the hemoglobin solution.[37] Therefore, HNTs are superior to other nanoparticles in view of clotting ability.

Generally, the clotting behavior of wound dressing is related to the chemical composition, morphological features, and 3D microstructure of the materials. Chitosan is a hemostat, which can help in natural blood clotting and blocks nerve endings and hence reduces pain. Chitosan's hemostasis ability can be attributed to the attraction of negatively charged residues on red blood cell membranes by protonated amine groups and the adsorption of fibrinogen and plasma proteins. On the other hand, HNTs are porous inorganic nanomaterials with hollow lumen structure, resulting in a high absorption ability for many types of active compounds. From the clotting experiment results, we can speculate that HNTs can shorten both the time lag for initial thrombin generation as well as the time to peak thrombin generation. Therefore, HNTs can accelerate the

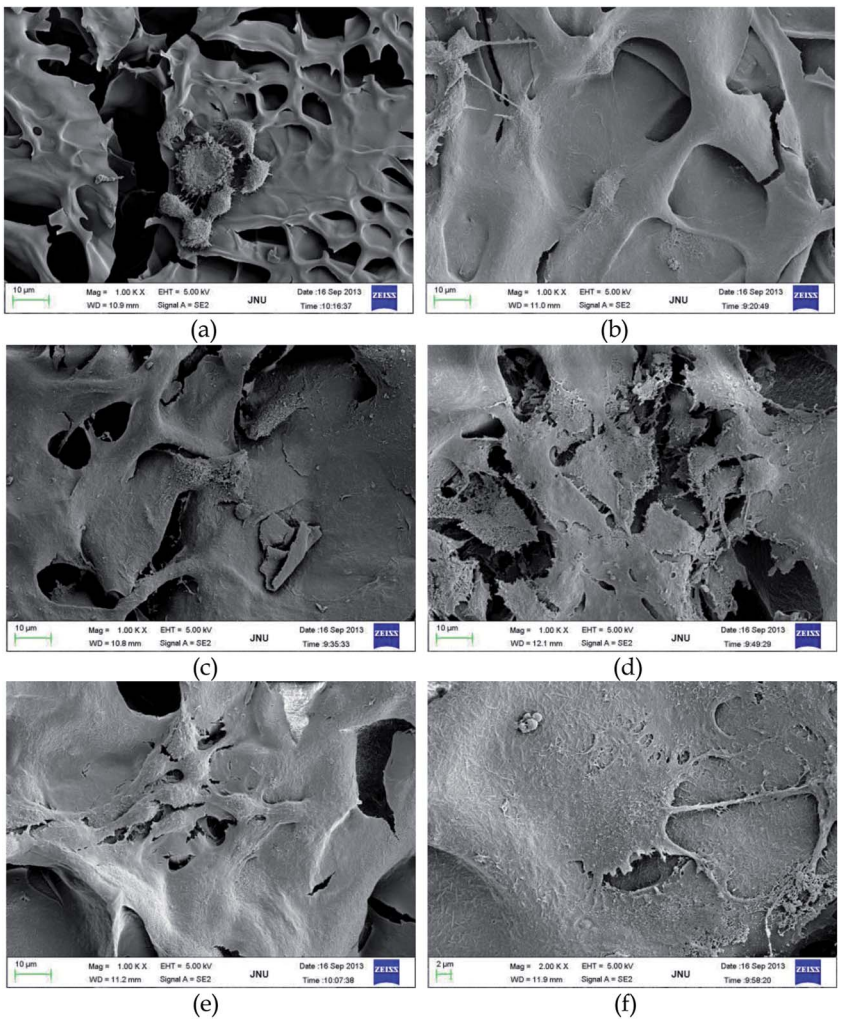

Fig. 9 SEM images of vascular endothelial cell cultured on CS–HNTs nanocomposite scaffolds after 3 days: (a) CS; (b) CS2N1; (c) CS1N1; (d) CS1N2; (e) CS1N4; (f) enlarged image of CS1N2 sample.

production of sufficient amounts of thrombin to support earlier fibrin generation. Due to the interactions between HNTs and chitosan and the 3D pore structures of the sponges, the composite sponges could trap more RBCs to enlarge and solidify the growing thrombus, leading to more rapid and stable clotting compared with pure chitosan. With respect to the HNTs powder, the low clotting ability can be attributed to the highly aggregated state of the tubes. The clotting ability of the sponges was further confirmed by the platelet adhesion experiment *via* the SEM observation (Fig. 7). It can be seen that the platelets exhibit spread morphology on the sponge surfaces, suggesting that the materials can activate platelets during wound healing.

Overall, the results of the hemostatic assays show that the CS1N2 sponges is the best among the samples for enhancing hemostasis, since it leads to the fastest blood clotting and platelet adhesion. Since the swelling ratio in PBS solutions by CS1N2 is comparable to that of pure chitosan, the enhanced blood absorption can be attributed to specific attractions of blood proteins and other blood components with HNTs. The ability of the composite sponges to absorb more blood should assist in stopping high flow hemorrhage and removing excess exudates at the wound interface.

3.5 Cell attachment and spread on the chitosan–HNTs composite sponges

The influence of HNTs on the cytocompatibility of chitosan sponges was assessed using the fibroblasts and endothelial cells. The morphology, adhesion, and spreading of the cells on pure chitosan and chitosan–HNTs composite sponges were observed by SEM as a result of the opacity of the composite films (Fig. 8 and 9). The two types of cells can spread on all of the samples after culturing for 3 days. SEM examination at higher magnification of the cell morphology (Fig. 8f) shows cellular extensions interacting closely with tubular HNTs in the composite sponges even when HNTs loading is as high as 80 wt%, indicating good cytocompatibility of the inorganic nanotubes. It can also be seen that the cells on the pure chitosan fail to spread completely. This is not a result from the possible toxicity of chitosan, but can be attributed to the smooth pore wall structures. From the morphology results above, the pore-walls of the composites are rougher than that of chitosan, therefore leading to the better spreading of the cells on them. The cell experiment results demonstrate a promotion effect of HNTs for the cell attachment and growth due to their high surface roughness of the composites and biocompatibility of HNTs. In our previous study, the cytocompatibility of HNTs was confirmed using the osteoblasts and fibroblasts in polyvinyl

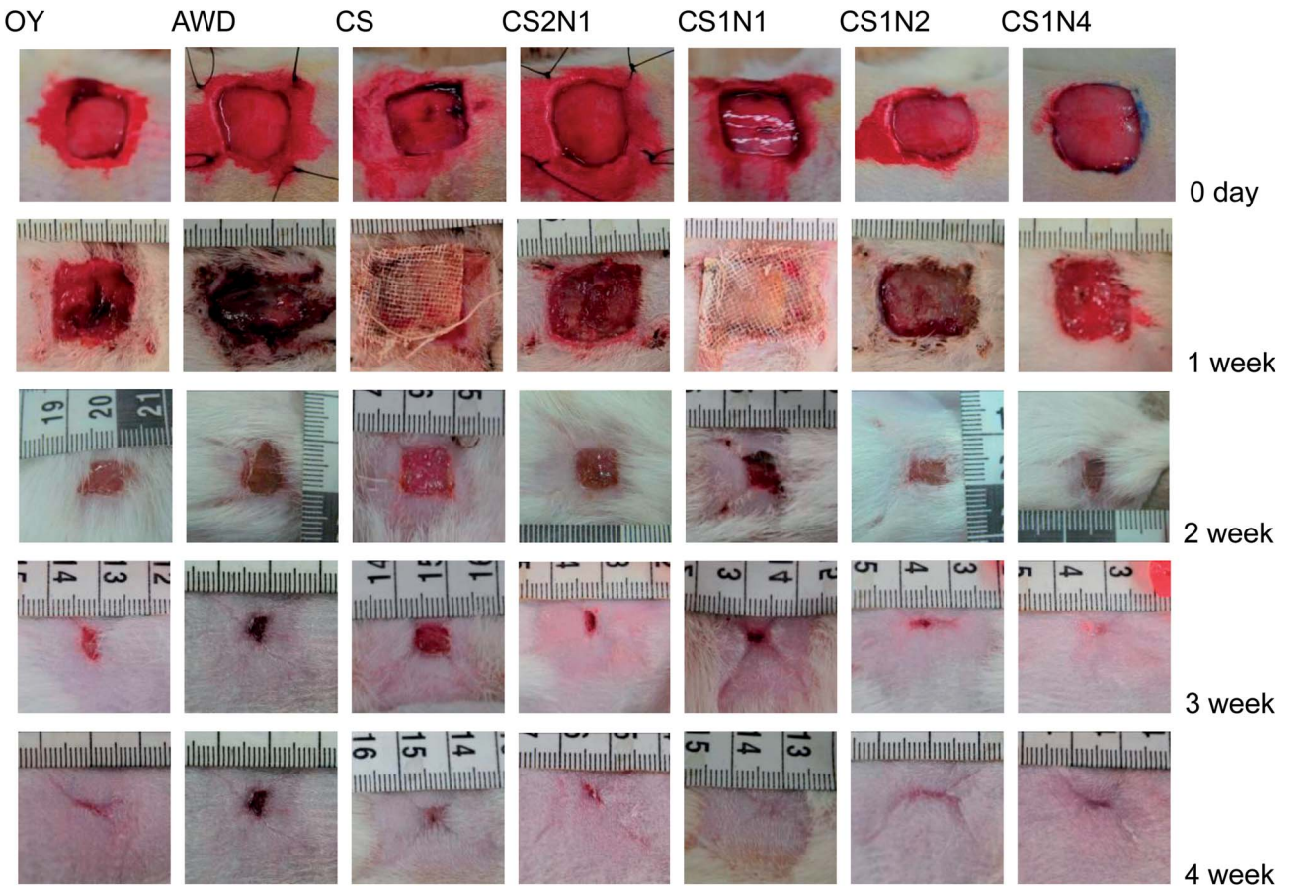

Fig. 10 Appearance of wounds treated with oily cotton gauze (OY), adhesive wound dressing (AWD), pure chitosan sponge, and chitosan–HNTs composite sponge.

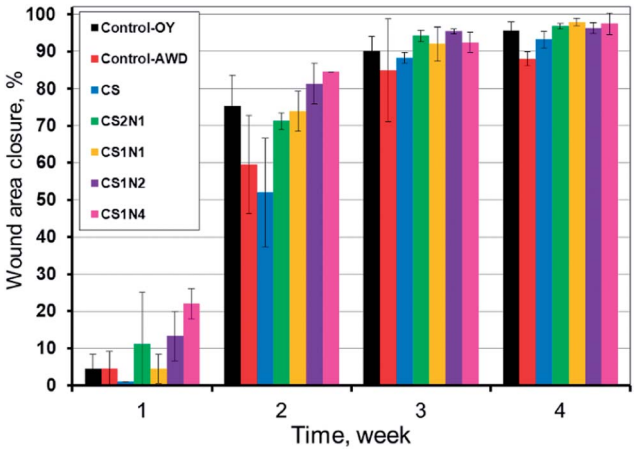

Fig. 11 Evaluation of the wound area closure treated by different dressing materials.

alcohol (PVA)–HNTs nanocomposites.[38] The morphological, physicochemical, blood-clotting properties and *in vitro* cell attachment and spread results of the chitosan–HNTs composite sponges indicate the possibility of them being used as wound dressing materials. These results stimulated us to evaluate their *in vivo* biological properties using full-thickness skin wound in an animal model.

3.6 *In vivo* wound healing evaluation of the chitosan–HNTs composite sponges

In vivo study conducted in SD rats demonstrates the enhanced wound healing ability of chitosan sponges by HNTs. Fig. 10 shows the images of the wound healing process after treatment with different materials. On the day of surgery, no visible difference in wound appearance is found. Obviously, for all the groups the wound shows granulation tissue formation with the extension of time. Except for the wounds treated by AWD, the wounds in the rats are nearly completely closed after a 4 week treatment. The regenerated skin is smooth and similar to normal skin without scar formation after 4 weeks, indicating the good healing ability for the skin tissue by the materials used. With respect to the differences among the groups, the unhealed area of the AWD group is much larger than that of other groups. Moreover, the composite sponges have much higher wound healing rate and contraction ability than those of pure chitosan sponges. The extent of wound closure was quantified at different time points and the results are shown in Fig. 11. After one week, the composite sponges show a 3.4–21-fold increase in closure ratio compared with the pure chitosan. Especially, the CS1N4 sponges show the highest closure ratio of 22%. After two weeks, apart from the AWD and OY groups, the wounds treated with the chitosan–HNTs composite sponges exhibit a linear increase in closure ratio with the loading of

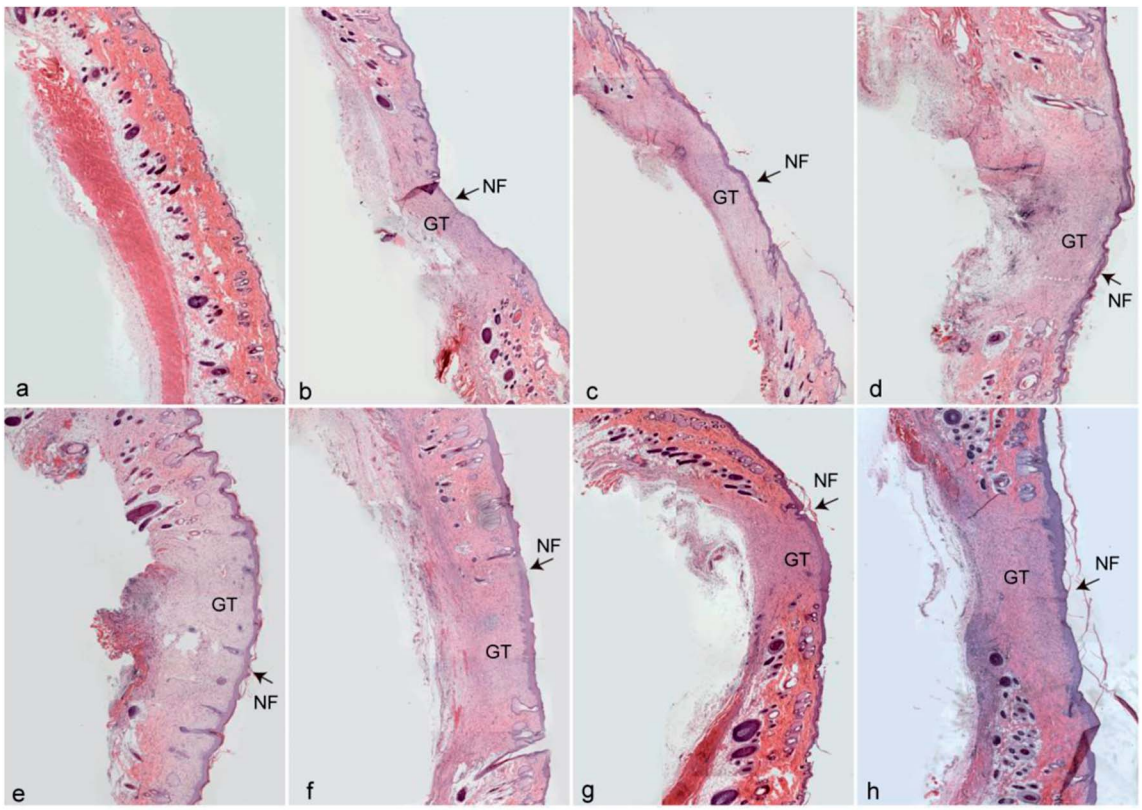

Fig. 12 Photomicrographs of hematoxylin and eosin (H&E)-stained normal skin (a), OY treated wounds (b), AWD treated wound (c), pure chitosan sponge treated wound (d), and chitosan–HNTs composite sponge treated wound ((e–h), (e) CS2N1; (f) CS1N1; (g) CS1N2; (h) CS1N4). The GT represents the granulation tissue and NE represents the neoepidermis.

HNTs. For example, the wound closure of CS1N4 sponges is ~85%, which is 32% higher than that of the pure chitosan sponges. For all groups, the data of closure after three and four weeks are slightly different, suggesting that wound healing is achieved after 3 weeks. The maximum closure at 28 day is 98.0%, which corresponds to the CS1N1 group. The data is substantially higher than that of pure chitosan groups, which is only 87%. It should also be noted that although OY can effectively repair the wound, the possibility of secondary damage upon removal limits their applications in skin regeneration.

From the *in vivo* healing experiment results, we can conclude that the incorporation of HNTs into chitosan can accelerate wound healing especially at the initial stage. This is attributed to the synergistic effect of chitosan and the HNTs. There are numerous reports on wound dressing materials based on chitosan.[25] The promotion of wound healing and scar prevention is realized by the stimulation of the inflammatory cell aggregation and promotion of the cell migration into the wound area by the porous scaffolds.[39] The improvement of wound healing ability of chitosan sponges by HNTs may be attributed to their intrinsic, high hemostasis properties and promotion of cell migration into the wound areas. In fact, the raw HNTs were commonly used as wound treatment materials in ancient China, although the mechanism for wound healing was not clear. The relevant mechanism will be discussed in the following section. Above all, the prepared wound dressing composite sponges have advantages such as rapid hemostasis, accelerated tissue regeneration, promoted cell attachment, and low cost. Furthermore, HNTs in the composite sponges can be used as a vehicle for biopharmaceuticals, antimicrobials, growth factors, and functional gene to wounds owing to their perfect lumen structures. From a practical point of view, the composite sponges are not dissolved or adhered to during the application period to the wound and are easy to remove without ripping the skin. Therefore, the chitosan–HNTs sponges have promising applications as wound dressing materials in skin or other organ regeneration.

3.7 Histological observation in the wound area

The final goal for the wound dressing of the skin is to restore the structural and functional properties to the levels of normal tissue, involving the re-epithelialization and orchestrated regeneration of all the skin appendages.[40] Fig. 12 shows the histological observations for the growth status and structure of epithelial tissue in each group at week 4 after the operation. It can be seen that for all the groups the wounds are closed without significant difference in the surrounding normal skin tissue. The areas of epithelialization and granulation tissues, including dense fibroblast deposition in the composite sponges groups, are found to be larger than those in AWD and OY groups. Re-epithelialization on the granulation tissue in open wound can form a barrier between the wound and the environment, which is very important for wound healing. The

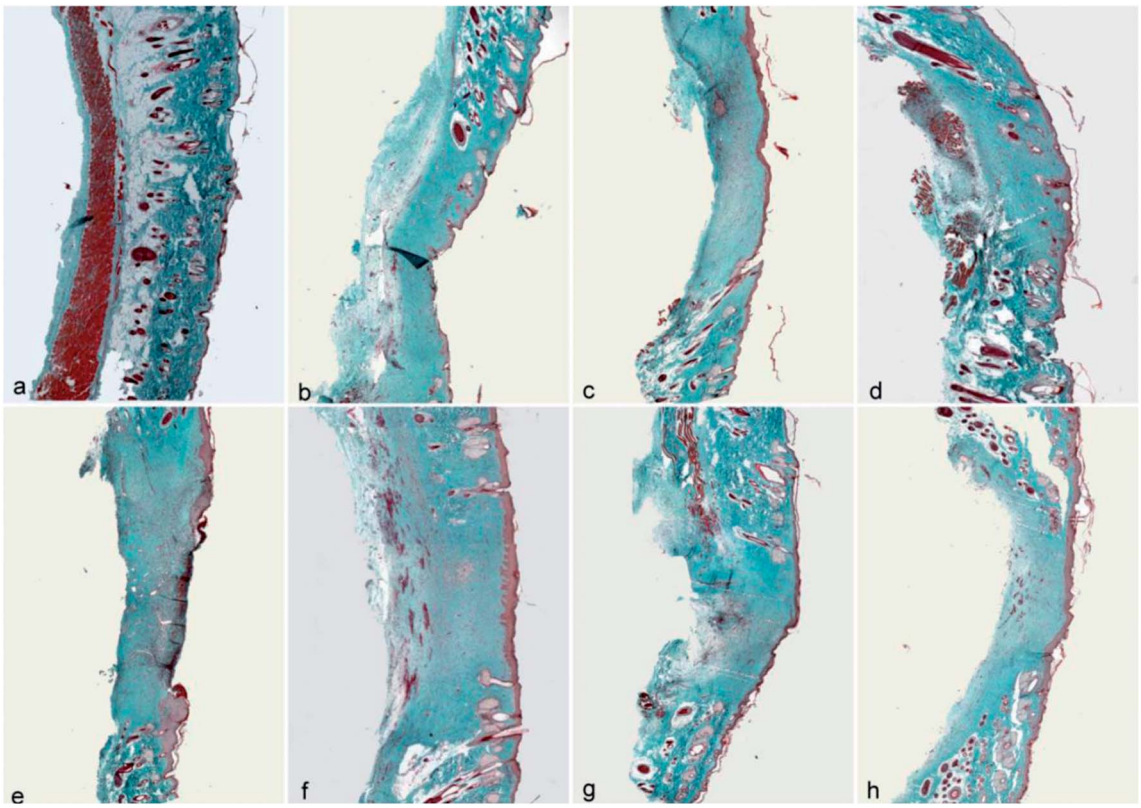

Fig. 13 Photomicrographs of Masson-stained normal skin (a), OY treated wounds (b), AWD treated wound (c), pure chitosan sponge treated wound (d), and chitosan–HNTs composite sponge treated wound ((e–h), (e) CS2N1; (f) CS1N1; (g) CS1N2; (h) CS1N4).

epithelialization rate and the deposition of collagen in the dermis are increased by HNTs. The wound treated by the CS1N2 sponge shows the minimum wound area among the various groups. Fully differentiated epidermic cells, closely arranged basal cells, and the horny layer and large amounts of hair and sebum are observed in the wound treated by the composite sponges, suggesting a similar epithelial structure to the normal skin. These results suggest HNTs can accelerate the proliferation of neonatal granulation tissue and offer optimum conditions for epithelial cell migration during wound healing, as well as the production of collagen by fibroblasts.

As shown in the HE staining results above, collagen deposition is observed in all the groups. Moreover, the amount and the type of collagen fibers are important for the keloids and hypertrophic scar formation. In the present study, Masson and SR staining were used to analyse the collagen deposition and remolding in the regenerated tissues. Fig. 13 shows the Masson staining images of the wound for different groups, in which red denotes keratin and muscle fibers, blue or green denotes collagen and bone, light red or pink denote cytoplasm, and dark brown or black denotes cell nuclei. The collagen fibers are fine and matured in the wound treated by the composite sponges, and their arrangement is similar to that of native skins. Fig. 14 shows the polarizing microscope images of collagen fibers by SR staining, in which the yellow/red color denotes collagen type I, red/white denotes collagen II, green denotes collagen type III and light yellow denotes collagen type IV. It can be seen that the type I collagen is the main component for the native skin. At week 4 after operation, the regenerated tissue in all the groups consists chiefly of collagen type I with a small amount of other types of collagen interspersed in the tissue, which is close to the profile of native skin. This also suggests the good healing ability of the composite sponges as well as the chitosan sponges.

Wound healing is a complex process, which consists of a series of coordinated overlapping biological events, involving acute and chronic inflammations, cell division, and extracellular matrix (ECM) synthesis. From the histological studies by the different staining, expect the AWD, all dressing materials exhibit good healing ability for the wound. Especially, the chitosan–HNTs composite sponges show improved wound healing ability. The mechanisms involved in beneficial healing activity should be attributed to the unique characteristics of HNTs. HNTs in the composite markedly increase the nano-roughness of the pore-wall for the sponges, which could (i) favor the trapping of factors detrimental to the repair process when present in excess (such as proteases, or reactive oxygen species), (ii) stimulate the progressive release of active fragments, which are reported to recruit and activate leukocytes and mesenchymal cells, and (iii) increase the surface available for protein coating and cell adhesion. Moreover, the enhancement in the mechanical property of the chitosan sponges by HNTs strongly regulates the phenotype and the differentiation process of the cells. In short, the highly porous structure and good mechanical properties of the chitosan–HNTs composite sponges allow

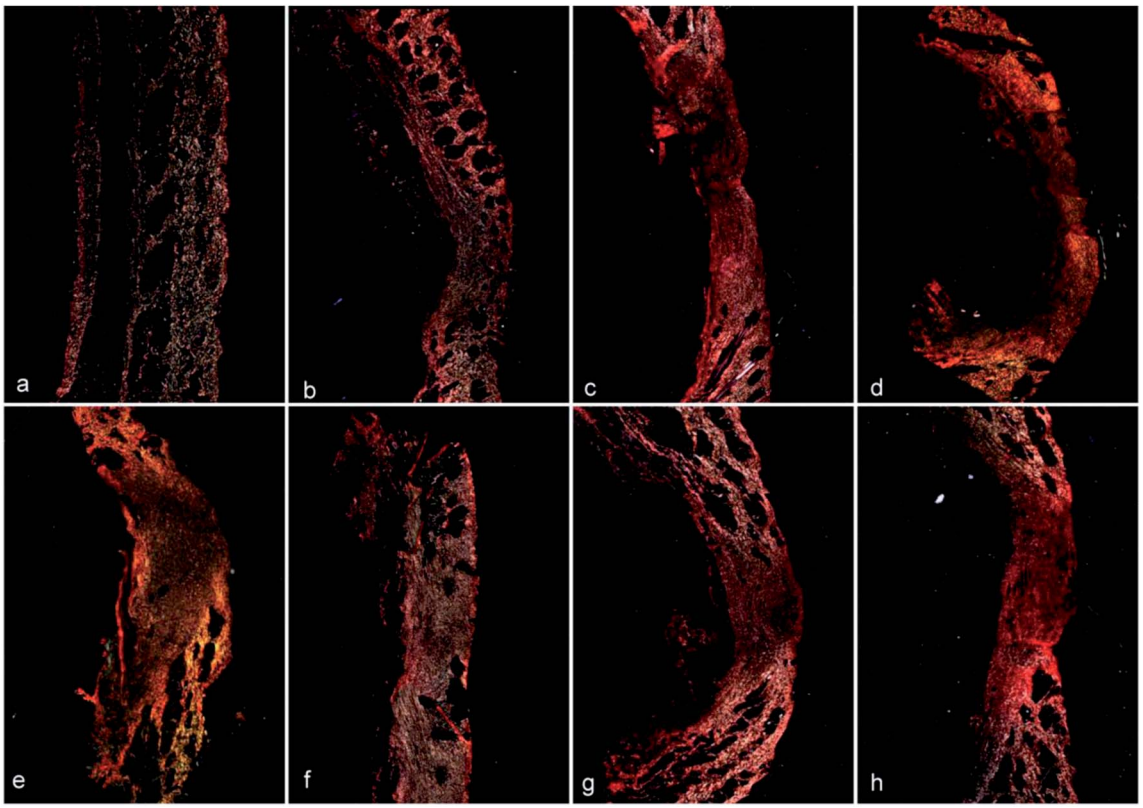

Fig. 14 Polarimicroscope images of SR-stained normal skin (a), OY treated wounds (b), AWD treated wound (c), pure chitosan sponge treated wound (d), and chitosan–HNTs composite sponge treated wound ((e–h), (e) CS2N1; (f) CS1N1; (g) CS1N2; (h) CS1N4).

gaseous and fluid exchanges, stop bleeding and absorb excess exudates, facilitate the attachment and spread of the cells, and promote the healing of the wounds, indicating that they are one of the most suitable wound dressing materials. Among the samples, the CS1N2 sponges with 33 wt% chitosan and 66 wt% HNTs exhibit the best overall performance. They show an 89.0% increase in clotting ability and 12%, 29.3%, 7.1% and 3.1% increase in the wound closure ratio after 1, 2, 3, and 4 weeks, respectively, compared with those of the pure chitosan sponges.

4. Conclusions

The chitosan–HNTs composite sponges with different HNTs loadings are prepared by lyophilization. The addition of HNTs slightly affects the pore structure of the chitosan sponges even with 80 wt%. A slight decreasing trend in porosity and weight loss in PBS of the composite sponges is obtained with the incorporation of the HNTs. The swelling ratios of the pure chitosan and chitosan–HNTs sponges in PBS solutions are comparable. HNTs can simultaneously enhance the elastic modulus, compressive strength, and toughness of the chitosan sponges. The fibroblasts and endothelial cells can spread well in the composite sponges, indicating their good cytocompatibility. The composite sponges show enhanced blood clotting and platelet activation ability. The composite sponges with 67% HNTs show an 89.0% increase in clotting ability compared with that of pure chitosan. *In vivo* wound healing evaluation confirms the enhanced healing ability of the chitosan sponges by HNTs. The composite sponges show a 3.4–21-fold increase in wound closure ratio compared with that of pure chitosan after one week. The addition of HNTs helps in faster re-epithelialization and collagen deposition. All these are attributed to the unique characteristics of HNTs and the synergistic effect of chitosan and the HNTs. Overall results demonstrate that these advanced chitosan–HNTs composite sponges have many potential applications for burn, chronic, and diabetic wound infections.

Acknowledgements

This work was financially supported by the National Natural Science Foundation of China (81272222), the Guangdong natural science funds for distinguished young scholar (S2013050014606), the foundation for the author of Guangdong excellent doctoral dissertation (sybzzxm201220), Guangdong science and technology project (2011B031300026), Guangzhou science and technology project (2013J4100099), Guangzhou applied basic research project (2013J4100100), the project of regional demonstration for Guangdong ocean economic innovative development (GD2012-B03-009), the research fund for the doctoral program of higher education of China (20114401120003), and the key project of department of education of Guangdong province (cxzd1108). The authors also thank Dr Hau-To Wong for reading and revising of the manuscript.

References

1 M. Ishihara, K. Nakanishi, K. Ono, M. Sato, M. Kikuchi, Y. Saito, H. Yura, T. Matsui, H. Hattori, M. Uenoyama and A. Kurita, *Biomaterials*, 2002, **23**, 833.
2 B. Balakrishnan, M. Mohanty, P. R. Umashankar and A. Jayakrishnan, *Biomaterials*, 2005, **26**, 6335.
3 M. S. Khil, D. I. Cha, H. Y. Kim, I. S. Kim and N. Bhattarai, *J. Biomed. Mater. Res., Part B*, 2003, **67**, 675.
4 F. L. Mi, S. S. Shyu, Y. B. Wu, S. T. Lee, J. Y. Shyong and R. N. Huang, *Biomaterials*, 2001, **22**, 165.
5 K. Ulubayram, A. N. Cakar, P. Korkusuz, C. Ertan and N. Hasirci, *Biomaterials*, 2001, **22**, 1345.
6 L. Huang, K. Nagapudi, R. P. Apkarian and E. L. Chaikof, *J. Biomater. Sci., Polym. Ed.*, 2001, **12**, 979.
7 S. Agarwal, J. H. Wendorff and A. Greiner, *Polymer*, 2008, **49**, 5603.
8 J. S. Boateng, K. H. Matthews, H. N. E. Stevens and G. M. Eccleston, *J. Pharm. Sci.*, 2008, **97**, 2892.
9 M. Kumar, *React. Funct. Polym.*, 2000, **46**, 1.
10 E. Khor and L. Y. Lim, *Biomaterials*, 2003, **24**, 2339.
11 H. Ueno, H. Yamada, I. Tanaka, N. Kaba, M. Matsuura, M. Okumura, T. Kadosawa and T. Fujinaga, *Biomaterials*, 1999, **20**, 1407.
12 F. Bergaya and G. Lagaly, *Handbook of Clay Science*, Elsevier, Oxford OX5 1GB, UK, 2nd edn, 2013.
13 D. Depan, A. P. Kumar and R. P. Singh, *Acta Biomater.*, 2009, **5**, 93.
14 Y. Lvov and E. Abdullayev, *Prog. Polym. Sci.*, 2013, **38**, 1690.
15 P. Luo, Y. F. Zhao, B. Zhang, J. D. Liu, Y. Yang and J. F. Liu, *Water Res.*, 2010, **44**, 1489.
16 R. R. Price, B. P. Gaber and Y. Lvov, *J. Microencapsulation*, 2001, **18**, 713.
17 M. Liu, C. Wu, Y. Jiao, S. Xiong and C. Zhou, *J. Mater. Chem. B*, 2013, **1**, 2078.
18 R. Qi, R. Guo, M. Shen, X. Cao, L. Zhang, J. Xu, J. Yu and X. Shi, *J. Mater. Chem.*, 2010, **20**, 10622.
19 M. Sirousazar, M. Kokabi and Z. M. Hassan, *J. Biomater. Sci., Polym. Ed.*, 2011, **22**, 1023.
20 S. T. Oh, W. R. Kim, S. H. Kim, Y. C. Chung and J. S. Park, *Fibers Polym.*, 2011, **12**, 159.
21 R. Huey, D. Lo and D. J. Burns, WO2008054566 A1, 2008.
22 Z. Xie, C. B. Paras, H. Weng, P. Punnakitikashem, L.-C. Su, K. Vu, L. Tang, J. Yang and K. T. Nguyen, *Acta Biomater.*, 2013, **9**, 9351.
23 M. Dai, X. Zheng, X. Xu, X. Kong, X. Li, G. Guo, F. Luo, X. Zhao, Y. Q. Wei and Z. Qian, *J. Biomed. Biotechnol.*, 2009, **2009**, 8.
24 S.-Y. Ong, J. Wu, S. M. Moochhala, M.-H. Tan and J. Lu, *Biomaterials*, 2008, **29**, 4323.
25 R. Jayakumar, M. Prabaharan, P. T. Sudheesh Kumar, S. V. Nair and H. Tamura, *Biotechnol. Adv.*, 2011, **29**, 322.
26 P. T. Sudheesh Kumar, V.-K. Lakshmanan, T. V. Anilkumar, C. Ramya, P. Reshmi, A. G. Unnikrishnan, S. V. Nair and R. Jayakumar, *ACS Appl. Mater. Interfaces*, 2012, **4**, 2618.

27 M. Liu, Y. Zhang, C. Wu, S. Xiong and C. Zhou, *Int. J. Biol. Macromol.*, 2012, **51**, 566.
28 Y. Xu, X. Ren and M. A. Hanna, *J. Appl. Polym. Sci.*, 2006, **99**, 1684.
29 X. Cheng, Y. Li, Y. Zuo, L. Zhang, J. Li and H. Wang, *Mater. Sci. Eng., C*, 2009, **29**, 29.
30 D. O. Costa, P. D. H. Prowse, T. Chrones, S. M. Sims, D. W. Hamilton, A. S. Rizkalla and S. J. Dixon, *Biomaterials*, 2013, **34**, 7215.
31 A. Singer, M. Zarei, F. M. Lange and K. Stahr, *Geoderma*, 2004, **123**, 279.
32 M. T. Qurashi, H. S. Blair and S. J. Allen, *J. Appl. Polym. Sci.*, 1992, **46**, 255.
33 L. J. Sweetman, S. E. Moulton and G. G. Wallace, *J. Mater. Chem.*, 2008, **18**, 5417.
34 R. Jayakumar, R. Ramachandran, V. V. Divyarani, K. P. Chennazhi, H. Tamura and S. V. Nair, *Int. J. Biol. Macromol.*, 2011, **48**, 336.
35 A. W. Seifert, S. G. Kiama, M. G. Seifert, J. R. Goheen, T. M. Palmer and M. Maden, *Nature*, 2012, **489**, 561.
36 P. T. S. Kumar, V.-K. Lakshmanan, M. Raj, R. Biswas, T. Hiroshi, S. Nair and R. Jayakumar, *Pharm. Res.*, 2013, **30**, 523.
37 B. S. Anisha, D. Sankar, A. Mohandas, K. P. Chennazhi, S. V. Nair and R. Jayakumar, *Carbohydr. Polym.*, 2013, **92**, 1470.
38 W. Y. Zhou, B. C. Guo, M. X. Liu, R. J. Liao, A. B. M. Rabie and D. M. Jia, *J. Biomed. Mater. Res., Part A*, 2009, **93**, 1574.
39 T. H. Dai, M. Tanaka, Y. Y. Huang and M. R. Hamblin, *Expert Rev. Anti-Infect. Ther.*, 2011, **9**, 857.
40 Y. Yang, T. Xia, F. Chen, W. Wei, C. Liu, S. He and X. Li, *Mol. Pharm.*, 2012, **9**, 48.